Turk J Chem
31 (2007) , 415 – 426.

Activation of Light Alkanes on Pure and Fe and Al Doped Silica Clusters: A Density Functional and ONIOM Study

Mehmet Ferdi FELLAH, Işık ÖNAL*
Department of Chemical Engineering, Middle East Technical University, Ankara, 06531-TURKEY
e-mail: ional@metu.edu.tr

Received 23.03.2007

C-H bond activation was studied by use of density functional theory (DFT) and ONIOM calculations as implemented in Gaussian 2003 at the B3LYP level utilising 6-31G* as the basis set for Si, Al, and Fe atoms and 3-21G** as the basis set for O and H atoms. Relative energy profiles were determined for pure silica modeled by a Si_7O_{21} cluster and Fe and Al doped silica clusters via coordinate driving calculations. The activation barriers for C-H bond activation of methane and ethane decrease with the substitution of Fe on the silica surface, which theoretically demonstrates a favorable effect of Fe substitution on that surface. The activation energy barriers of methane and ethane are substantially decreased from the approximate transition state values of 55.14 kcal/mol and 54.89 kcal/mol for pure silica cluster to 33.43 kcal/mol and 36.54 kcal/mol obtained for the approximate transition state for Fe substituted silica, respectively.

Key Words: C-H bond activation, methane, ethane, silica, Fe doping, Al doping, density functional theory, DFT, ONIOM.

Introduction

During the past 2 decades, the C-H bond activation of small alkanes, which is considered the rate-limiting step in catalytic partial oxidation, has received a great deal of attention both experimentally and theoretically. Several authors have investigated partial and selective oxidations of methane by means of silica supported catalysts.[1−13] Arena et al.[10,11] investigated the kinetics of the partial oxidation of methane to formaldehyde on a silica catalyst. They reported that the rate-determining step is the activation of C-H bond of methane molecule. Silica based oxide catalysts signify a superior functionality in the methane partial oxidation (MPO) and several clues have been offered for relating the surface structure and the coordination of supported transition metal oxide species with their reactivity.[12] Yamada et al.[13] measured catalytic activity in terms of methane oxidation for 43 elements doped in silica prepared by an impregnation method. It was found

*Corresponding author

that Al and Fe substitution on silica increases the production rate of formaldehyde and methyl alcohol, Fe substitution being the most favorable one.

Several authors have studied the activation of methane on different metals by DFT methods.[14−17] Methane dissociation and syngas formation on a number of transition metals M (M = Ru, Os, Rh, Ir, Pd, Pt, Cu, Ag, Au) have been investigated by Tong et al.[14] The transition states of the elementary reactions for C-H activation of methane on a Ru(0001) surface was studied with DFT periodic calculations using the nudged elastic band (NEB) method by Ciobica et al.[15] Methane dissociative adsorption by means of DFT was investigated by Henkelman et al.[16] on an Ir(111) surface and by Bunnik et al.[17] on Rh(111).

Light alkane activation reactions on pure silica or on silica-supported metals have been investigated theoretically by several authors.[18−24] Adsorption sites of light alkanes on silicalites and activation barriers and mechanisms of dehydrogenation reactions were studied by molecular dynamics simulation techniques and DFT at B3LYP level of calculations using 6-31G** and 6-311G** basis sets.[18] Mota et al.[19] studied the activation of alkanes on zeolites, hydride abstraction, and dehydrogenation on extra-framework aluminum species by DFT B3LYP/6-31G(d,p) methods. It was shown that dehydrogenation has a significantly lower activation enthalpy, especially for linear alkanes. A quantum chemical study of alkane hydrogenolysis and metathesis on silica-supported Group VB metal hydrides (V, Nb, Ta) was done by DFT at B3LYP level by Mikhailov et al.[20−22] Their β-crystobalite silica surface was modeled as $(H_4Si_2O_5)(OH)_2$. Various metals were supported on this surface. Semiempirical quantum chemical methods to examine the partial oxidation reaction mechanisms and active sites on MgO and pure silica were employed by Önal and Şenkan[23] and Öztürk et al.[24] respectively.

Blaszkowski et al.[25] the investigated transition states and the corresponding energy barriers of the reactions related to C-H bond activation of dehydrogenation of ethane catalyzed by a protonated zeolite by DFT. The activation barrier computed was reported as 71 kcal/mol. Zheng et al.[26] researched the transition state structures and activation energies of ethane cracking and dehydrogenation reactions catalyzed by a zeolite model cluster by means of ab initio methods, HF and MP2. The influence of the zeolite cluster size and acidity was also studied quantitatively on ethane conversion reaction activation energies. The activation barrier was calculated to be 75.9 kcal/mol for this reaction. The DFT method was also utilized to study light alkane dehydrogenation on Ga-exchanged HZSM-5 by means of DFT at B3LYP level.[27] Two types of catalytic sites, a mono-Al site and a di-Al site, were considered to determine the activation barriers of C-H bond activation of ethane. The values of the activation barriers reported range from 85.7 to 38.4 kcal/mol. Pereira et al.[28] examined the dehydrogenation reaction of ethane in gallium containing zeolites using DFT with B3LYP. Two different mechanisms, a 3-step mechanism and a 1-step concerted mechanism, were considered during the dehydrogenation reaction of ethane. C-H activation of ethane according to σ-bond metathesis was studied on mononuclear Cr(III) surface sites on silica models by combined quantum mechanical–molecular mechanical (QM–MM) methods by Lillehaug et al.[29] The range of the calculated activation barrier was from 43 to 60 kcal/mol.

In this study, in order to observe the effect of Fe and Al doping on silica for C-H bond activation of methane and ethane, ONIOM-DFT/B3LYP calculations are used to obtain energy profiles and approximate transition states involved in C-H bond activation of methane catalyzed by a SiO_2 (low quartz) surface modeled by a Si_7O_{21} cluster and isomorphously substituted Fe and Al silica clusters.

Surface Models and Computational Method

Quantum chemical calculations employing DFT[30] are carried out to investigate the energetics of C-H bond activation of methane and ethane by pure silica, Al doped silica, and Fe doped silica clusters. All calculations are conducted using the Gaussian 2003 suite of programs.[31] DFT calculations are carried out using Becke's[32,33] 3-parameter hybrid method involving the Lee, Yang, and Parr[34] correlation functional (B3LYP) formalism. A 2-layer ONIOM method is used to simulate the pure SiO_2 (low quartz) surface modeled by a Si_7O_{21} cluster where 2 Si and 6 O atoms (8 atoms in total) are in the high layer DFT region and the rest of the clusters (20 atoms in total) are in the low layer molecular mechanics region utilizing a universal force field (UFF). Fe or Al was isomorphously substituted into this cluster for a high layer Si atom. At the bottom oxygen atom of the bridge, an H atom was used to obtain a total neutral charge for the Fe and Al doped silica clusters.[35] Figure 1 illustrates the 3 different silica clusters. Energy profile and transition state (TS) calculations were in general performed for the determination of activation barriers. The basis sets employed in DFT calculations are 6-31G* for Si, Al, and Fe atoms, and 3-21G** for O and H atoms as implemented in Gaussian 2003. All energies and energy differences are calculated for 0 K without zero point energy (ZPE) corrections. The ZPE corrections would likely be similar for each of these cluster systems and thus would not influence conclusions based on the relative energies.

The computational strategy employed in this study is as follows:

Initially, all of the clusters and the adsorbing molecules, methane and ethane, are fully optimized geometrically by means of the equilibrium geometry (EG) calculations. EG calculations for pure silica cluster and Al doped silica were obtained taking the total charge as neutral, and spin multiplicity as a singlet, meaning there is no unpaired electron in the system. The total charge was neutral, and spin multiplicity was found to be 6, meaning there are 5 unpaired electrons in the system for the Fe doped silica cluster.

The adsorbing molecules, CH_4 and C_2H_6, are then located over the active site of the cluster at a selected distance and a coordinate driving calculation is performed by selecting a reaction coordinate in order to obtain the variation of the relative energy with a decreasing reaction coordinate to get an energy profile as a function of the selected reaction coordinate distance. Single point equilibrium geometry calculations were also performed where necessary by locating the adsorbing molecule in the vicinity of the catalytic cluster. Coordinate driving calculation results in an energy profile. The resulting relative energies for the cluster and reactant molecule complex are plotted against the reaction coordinate. The relative energy is calculated using the following formula:

$$\Delta E = E_{System} - (E_{Cluster} + E_{Adsorbate})$$

where E_{System} is the calculated energy of the given geometry containing the cluster and the adsorbing molecule at any distance, $E_{Cluster}$ is the energy of the cluster, and $E_{Adsorbate}$ is that of the adsorbing molecules, which are CH_4 and C_2H_6 in this work.

After obtaining the energy profile for the reaction, the geometry with the minimum energy on the energy profile is re-optimized by means of EG calculations to obtain the final geometry for the reaction. In this re-optimization calculation, there is no reaction coordinate that is fixed. Additionally, from the energy profile, the geometry with the highest energy is taken as the input geometry for the transition state geometry calculations. Starting from these geometries, the transition state structures with only one negative eigenvalue in the Hessian matrix are obtained. If a successful transition state geometry cannot be achieved,

the geometry with the maximum energy in the energy profile is reported as the approximate transition state geometry.

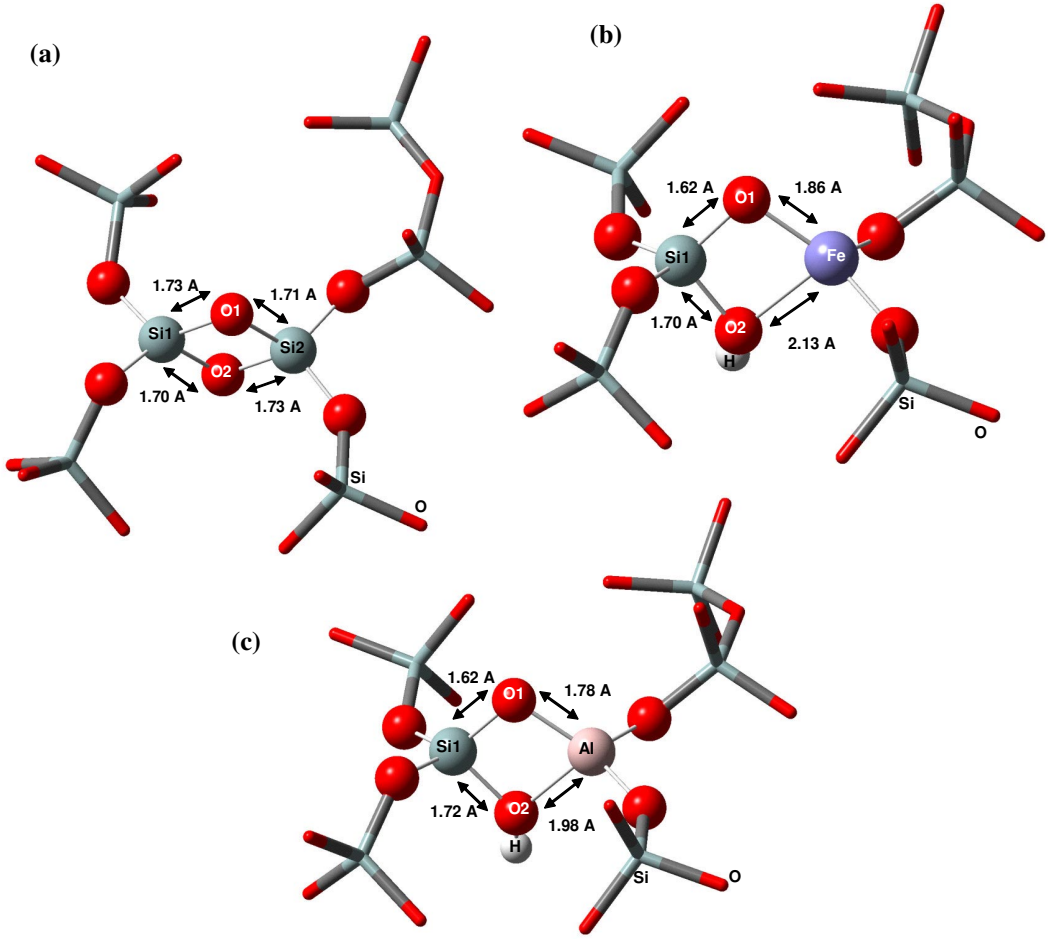

Figure 1. Optimized equilibrium geometries (EGs): a) Pure silica cluster, b) Fe doped silica cluster, c) Al doped silica cluster. High layer (DFT region) is represented by ball-bond view and low layer (molecular mechanics region) is represented by tube view.

Results

A. Optimized Geometries of Clusters

EGs for methane and ethane as reactant molecules were obtained by taking the total charge to be neutral and with a singlet spin multiplicity. Table 1 gives the calculated C-H bond distance value of 1.093 A and H-C-H angle value of 109.47° of methane molecule which are close to the previously reported experimental[36] values of 1.096 A and 109.50°, respectively. The calculated C-H bond distance value of 1.095 A and C-C bond distance value of 1.530 A of ethane molecule are close to the previously reported experimental[36] values of 1.091 A and 1.536 A, respectively. The calculated H-C-H angle value of 108.04° and H-C-C angle value of 110.87° of ethane molecule are close to the experimental[36] values of 108.45° and 110.90°, respectively.

The EGs for the pure silica, Fe doped silica, and Al doped silica clusters are represented in Figure 1. The calculated Si-O bond distance values of 1.65 A to 1.73 A were close to the reported bulk experimental[37]

values of 1.61 A - 1.74 A. O-H distances are 0.96 A. Fe-O distances for Fe doped cluster vary from 1.86 to 2.13 A and Al-O distances for Al doped cluster range from 1.77 A to 1.99 A.

Table 1. Comparison of calculated geometric values of methane and ethane with literature values.

	Methane		Ethane	
Bond Length, A	This Work	Exp[36]	This Work	Exp[36]
C-H	1.093	1.096	1.095	1.091
C-C	-	-	1.530	1.536
Angle, °				
H-C-H	109.47	109.50	108.04	108.45
H-C-C	-	-	110.87	110.90

B. Activation of Methane

Activation of a C-H bond of methane on a pure silica cluster was energetically examined and the energy profile for this reaction was obtained as shown in Figure 2. The reaction coordinate was selected as the distance between one of the hydrogen atoms of the methane (H1) and the active site of the cluster (O1). Other possible reaction coordinate calculations such as the one between a hydrogen atom of methane and other possible active sites such as Si, Al, or Fe or between the carbon atoms of methane and Si, Al, Fe, or O were also done. However, relative energies of these reactions were found to be too high and they were considered unfavorable.

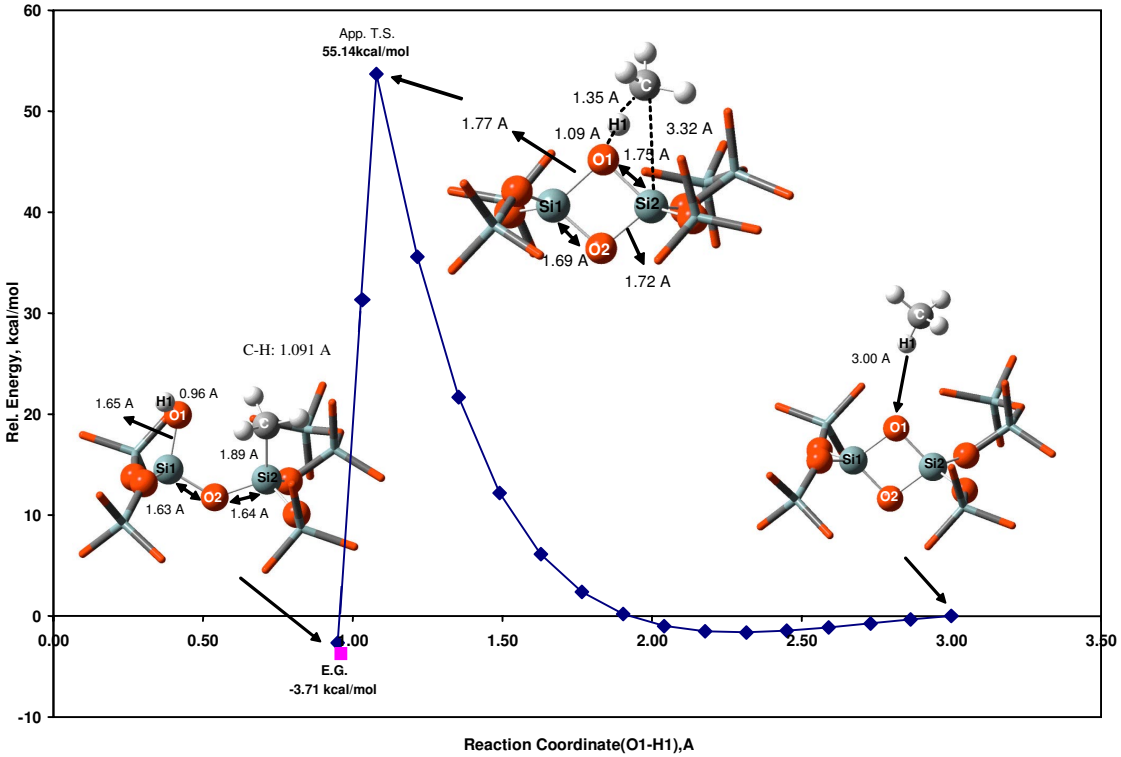

Figure 2. Methane activation on a pure silica cluster; High layer (DFT region) is represented by ball-bond view and low layer (molecular mechanics region) is represented by tube view.

The system consisting of the cluster and the methane molecule was considered neutral with a singlet spin multiplicity for all the calculations. Computations indicate that methane first physically adsorbs on the cluster and then the bridge is broken, leading to carbonium ion (CH_3^+) formation on the cluster as can be observed in Figure 2. The physical adsorption energy of methane on a pure silica cluster is generally observed to be a small value (-1.62 kcal/mol for this case). An approximate transition state barrier for C-H bond activation is calculated to be 55.14 kcal/mol. The energy profile for the activation of a C-H bond of methane on an Al doped silica cluster is shown in Figure 3. For this case the physical adsorption energy of methane on the Al doped silica cluster is found to be 2.76 kcal/mol. An approximate transition state barrier for C-H bond activation is calculated to be 53.09 kcal/mol.

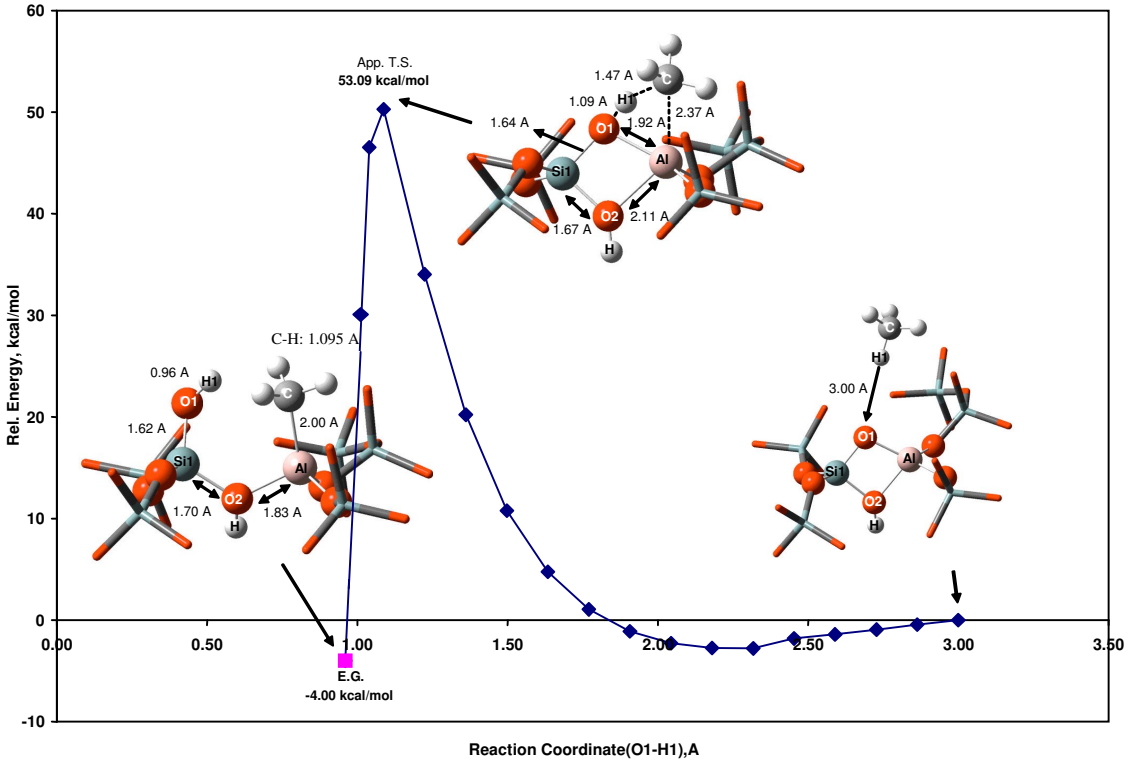

Figure 3. Methane activation on an Al doped silica cluster. High layer (DFT region) is represented by ball-bond view and low layer (molecular mechanics region) is represented by tube view.

Figure 4 gives the energy profile of activation of a C-H bond of methane on an Fe doped silica cluster. The physical adsorption energy of methane on the Fe doped silica cluster is 2.64 kcal/mol. The approximate activation barrier that was obtained by means of a transition state calculation is 33.43 kcal/mol.

C. Activation of Ethane

Activation of a C-H bond of ethane on a pure silica cluster was energetically examined and the energy profile for this reaction was obtained as shown in Figure 5. The reaction coordinate was selected as the distance between one of the hydrogen atoms of the ethane (H1) and the active site of the cluster (O1). Other possible reaction coordinate calculations such as the one between a hydrogen atom of ethane and other possible active

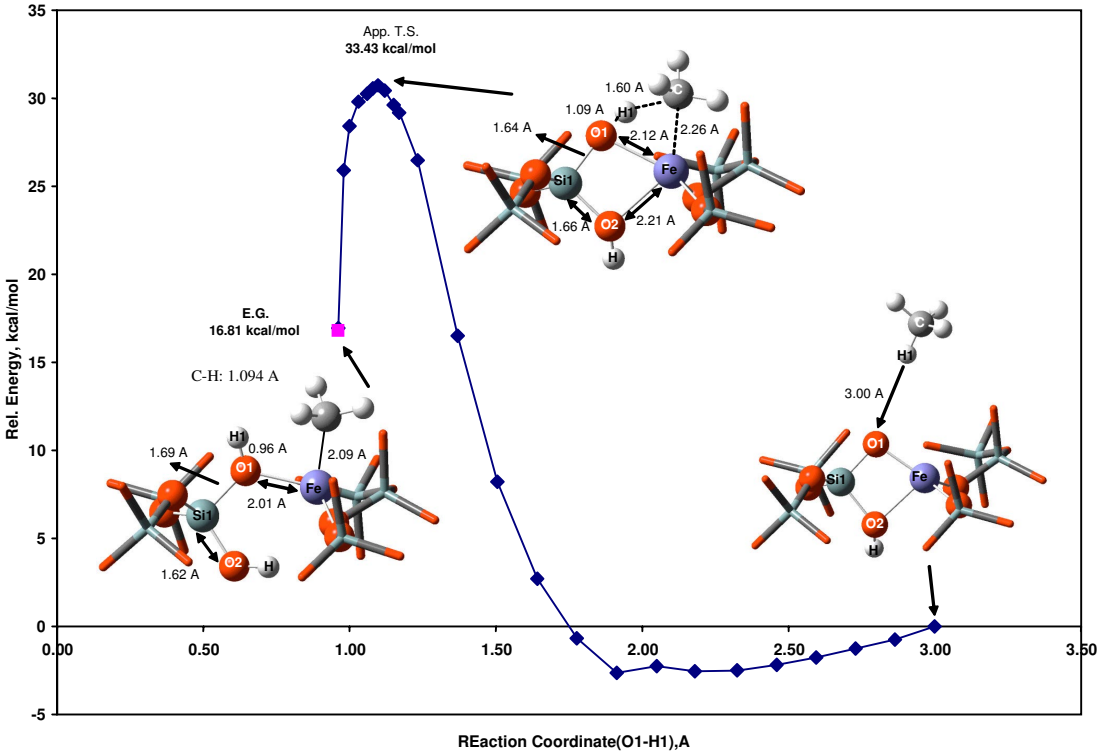

Figure 4. Methane activation on an Fe doped silica cluster; High layer (DFT region) is represented by ball-bond view and low layer (molecular mechanics region) is represented by tube view.

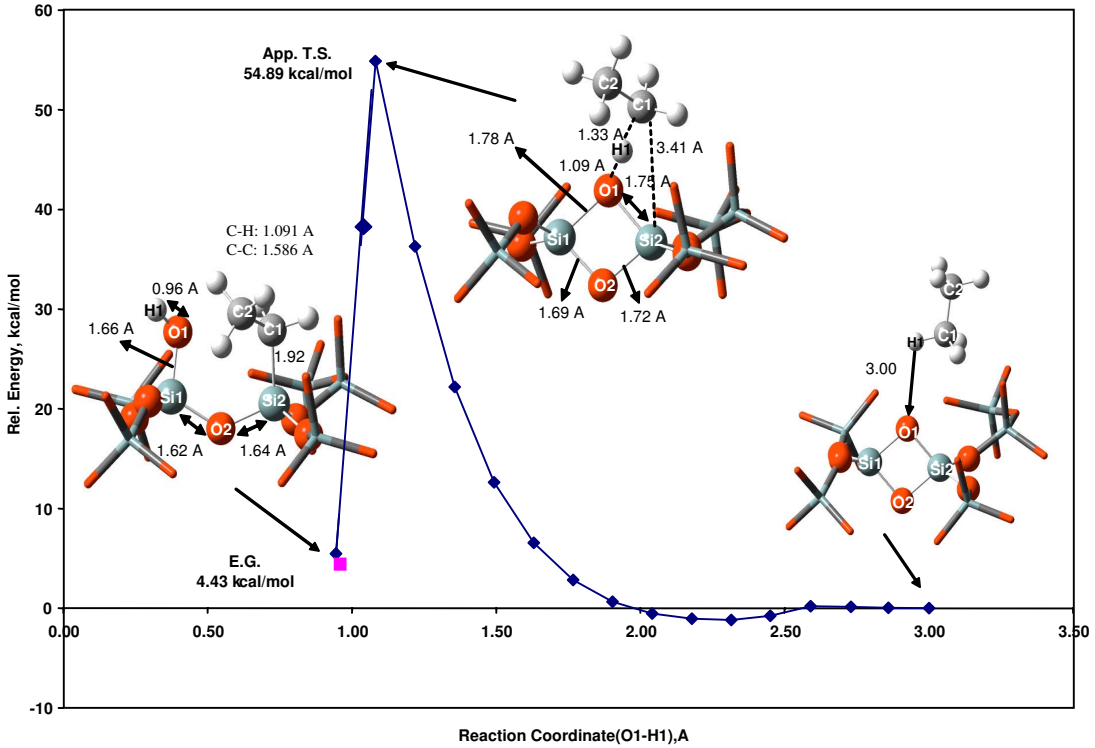

Figure 5. Ethane activation on a pure silica cluster; High layer (DFT region) is represented by ball-bond view and low layer (molecular mechanics region) is represented by tube view.

sites such as Si, Al, or Fe or between a carbon atom of ethane and Si, Al, Fe, or O were also done. However, relative energies of these reactions were found to be too high and they were considered unfavorable. It is also already well known that it is more difficult to break a C-H bond than a C-C bond.[25,38] The system consisting of the cluster and the ethane molecule was considered neutral with a singlet spin multiplicity for all the calculations. Computations again indicate that ethane first physically adsorbs on the cluster and then the bridge is broken leading to carbonium ion ($CH_3CH_2^+$) formation on the cluster as can be observed in Figure 5. The physical adsorption energy of ethane on a pure silica cluster is calculated to be 1.15 kcal/mol. An approximate transition state barrier for C-H bond activation is calculated to be 54.89 kcal/mol.

The energy profile for the activation of a C-H bond of ethane on an Al doped silica cluster is shown in Figure 6. For this case the physical adsorption energy of ethane on an Al doped silica cluster is found to be 0.97 kcal/mol. An approximate transition state barrier for C-H bond activation is calculated to be 53.35 kcal/mol.

Figure 7 gives the energy profile of the activation of a C-H bond of ethane on a Fe doped silica cluster. The physical adsorption energy of ethane on the Fe doped silica cluster is only 0.15 kcal/mol. The activation barrier that was obtained by means of an approximate transition state calculation is 36.54 kcal/mol.

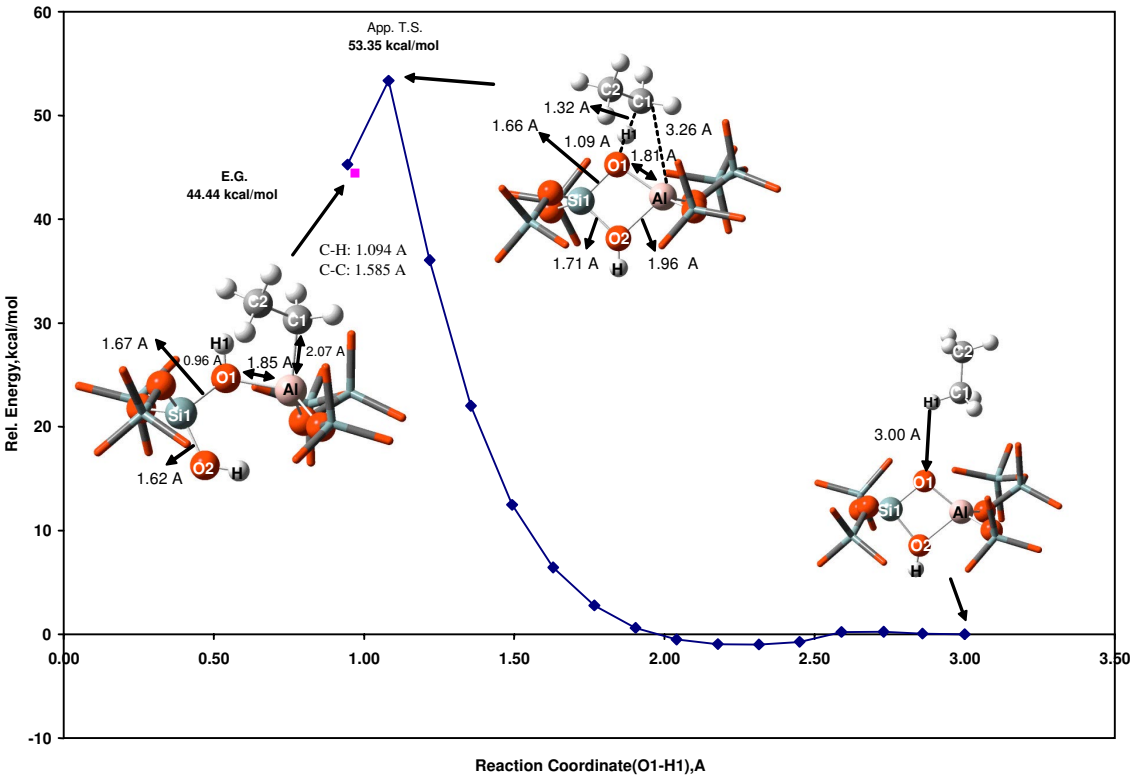

Figure 6. Ethane activation on an Al doped silica cluster; High layer (DFT region) is represented by ball-bond view and low layer (molecular mechanics region) is represented by tube view.

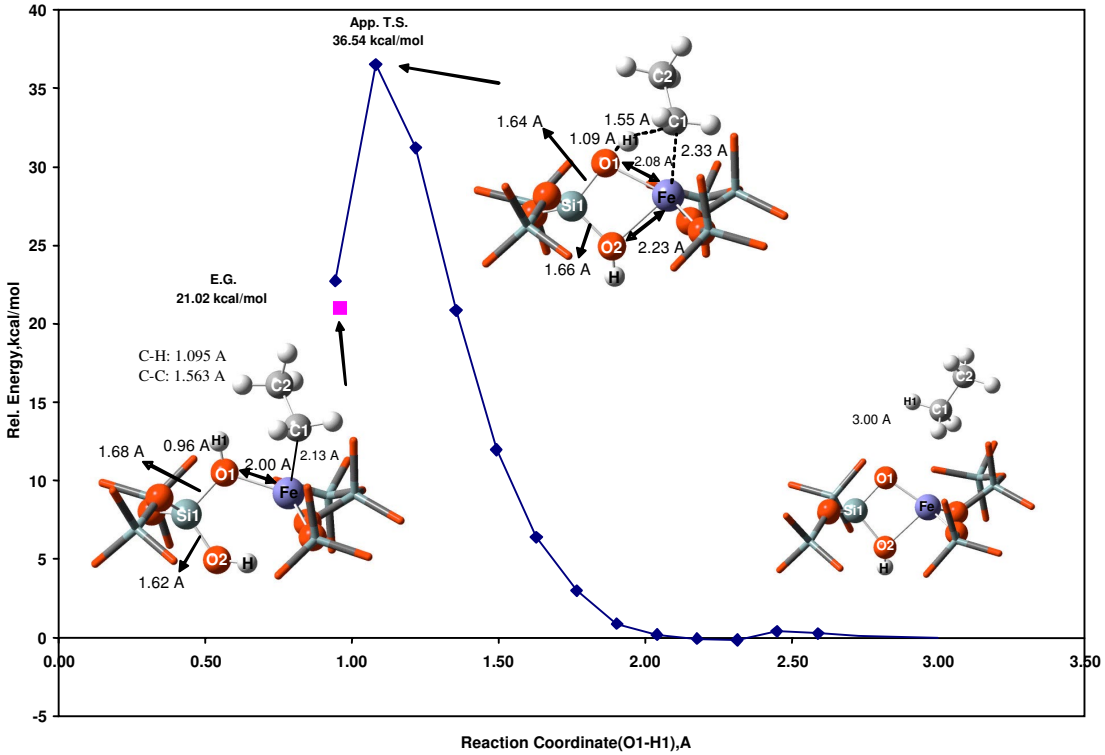

Figure 7. Ethane activation on a Fe doped silica cluster; High layer (DFT region) is represented by ball-bond view and low layer (molecular mechanics region) is represented by tube view.

Table 2. Calculated activation barriers of methane and ethane activation.

	Methane activation			Ethane activation		
	Pure silica cluster	Al doped silica cluster	Fe doped silica cluster	Pure silica cluster	Al doped silica cluster	Fe doped silica cluster
Activation barrier, kcal/mol	55.14	53.09	33.43	54.89	53.35	36.54

Discussion

The activation barrier values for methane and ethane molecules decrease drastically by doping Fe on a pure silica cluster. Fe doping decreases the activation barrier of C-H bond activation of methane and ethane significantly. Figures 8 and 9 and Table 2 give this comparison in detail.

In conclusion the favorable effects of Fe substitution on a silica surface have been demonstrated theoretically for C-H bond activation of both methane and ethane. The activation barriers substantially decrease with substitution of Fe on a silica cluster. Since the rate-determining step of MPO is generally agreed to be the C-H bond activation of methane,[10,11] our theoretical methane activation ranking results, given in Figure 8, are in relatively good agreement with the experimental catalytic ranking data of the partial oxidation of methane given in Figure 10. In this figure, the experimental rankings of the catalysts[13] for methane partial oxidation on Al and Fe doped silica catalysts are compared. The reaction conditions are

CH_4/O_2= 90/10, GHSV = 4760 h^{-1} and T = 773 K. Under these conditions, pure silica has no experimental catalytic activity. Fe doped silica catalyst has a larger production rate of MeOH and HCHO than the Al doped silica cluster, which is in agreement with the theoretical activity ranking of the catalyst clusters by use of activation barrier results obtained in our work.

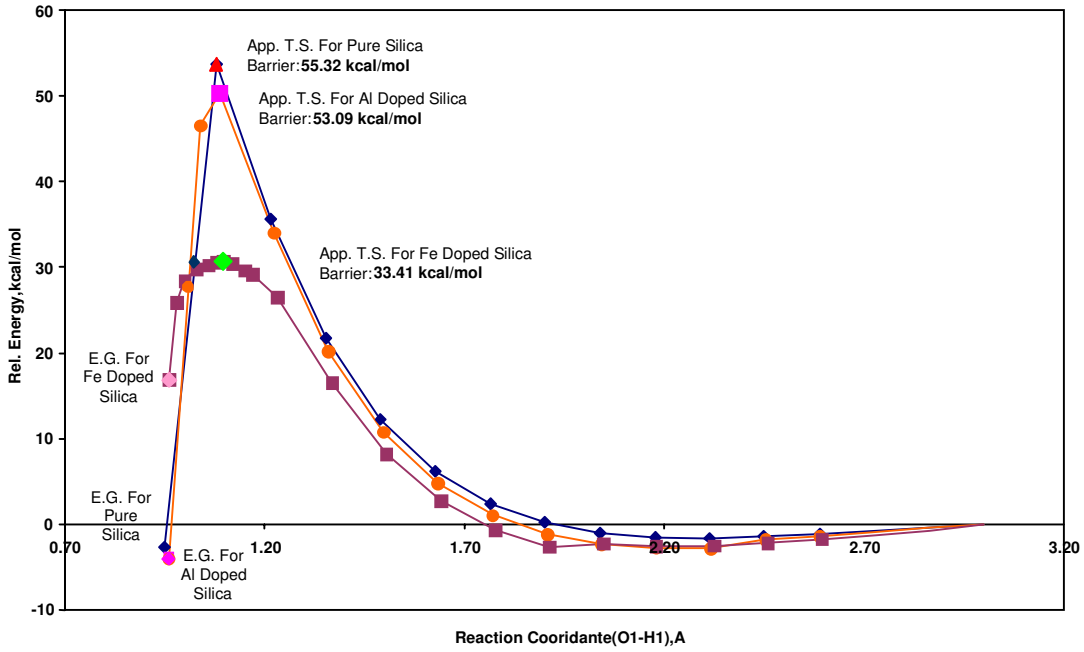

Figure 8. A comparison of methane C-H bond activation energy profile for various catalytic clusters.

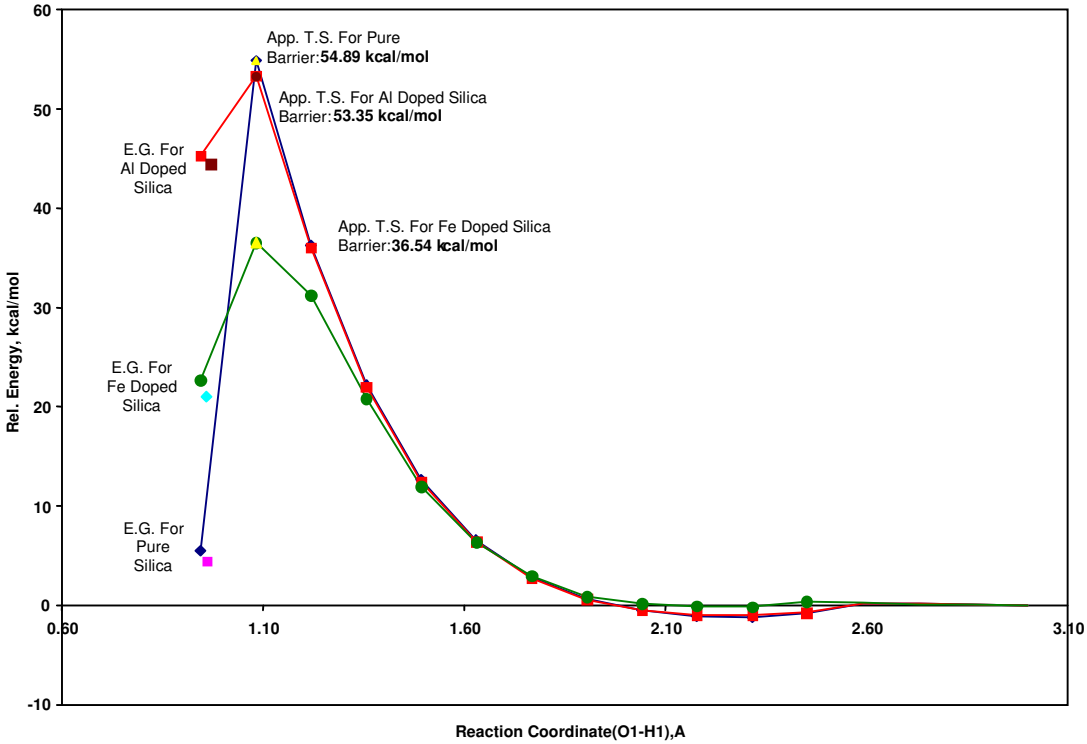

Figure 9. A comparison of ethane C-H bond activation energy profile for various catalytic clusters.

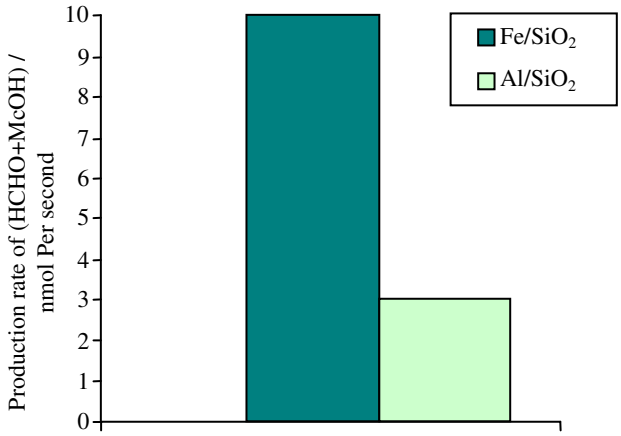

Figure 10. Experimental production rate of methane partial oxidation for Al and Fe substituted silica catalysts.[13]

References

1. Z. Zhaoa and T. Kobayashi, **Applied Catalysis A: General 207**, 139-149 (2001).
2. K. Nakagawa, Y. Teng, Z. Zhao, Y. Yamada Y.A. Ueda, T. Suzuki and T. Kobayashi, **Catal. Lett. 63**, 79-82 (1999).
3. Z. Zhao, Y. Yamada, Y. Teng, A. Ueda, K. Nakagawa and T. Kobayashi, **J. Catal. 190**, 215-227 (2000).
4. X. Ge, M. Zhu and J. Shen, **React. Kinet. Catal. Lett. 77**, 103-108 (2002).
5. T. Kobayashi, **Catalysis Today 71**, 69-76 (2001).
6. A.V. Kucherov, A.V. Ivanov, T.N. Kucherova, V.D. Nissenbaum and L.M. Kustov, **Catal. Today 81**, 297-305 (2003).
7. R. Grabowski and J. Słoczynski, **Chemical Eng. and Processing 44**, 1082-1093 (2005).
8. B. Silberova, M. Fathi and A. Holmen, **Applied Catalysis A: General 276**, 17-28 (2004).
9. E. Heracleous and A.A. Lemonidou, **Applied Catalysis A: General 269**, 123-135 (2004).
10. F. Arena, F. Frusteri and A. Parmaliana, **AIChE Journal 46**, 2285-2294 (2000).
11. F. Arena and A. Parmaliana, **Accounts of Chemical Research 36**, 867-875 (2003).
12. A. Parmaliana, F. Arena, F. Frusteri, A. Martínez-Arias M. Lopez Granados and J.L.G. Fierro, **Appl. Catal. A: Gen. 226**, 163-174 (2002).
13. 13. Y. Yamada, A. Ueda, H. Shioyama and T. Kobayashi, **Applied Catalysis A: General 254**, 45-58 (2003).
14. A.C. Tong, Fai Ng Ching and M. Sheng Liaoy, **Journal of Catalysis 185**, 12-22 (1999).
15. I.M. Ciobica, F. Frechard, R.A. van Santen, A.W. Kleyn and J. Hafner, **J. Phys. Chem. B 104**, 3364-3369 (2000).
16. G. Henkelman and H. Jónsson, **Physical Review Letters 86**, 664-667 (2001).
17. B.S. Bunnik and G. Jan Kramer, **Journal of Catalysis 242**, 309-318 (2006).

18. E.A. Furtado, I. Milas, J.O. Milam de Albuquerque Lins and M.A. Chaer Nascimento, **Phys. Stat. Sol. (a) 187**, 275-288 (2001).
19. C.J.A. Mota, D.L. Bhering and A. Ramirezsolis, **International Journal of Quantum Chemistry, 105**, 174-185 (2005).
20. M.N. Mikhailov, A.A. Bagatur'yants and L.M. Kustov, **Russian Chemical Bulletin, International Edition 52**, 30-35 (2003).
21. M.N. Mikhailov, A.A. Bagatur'yants and L.M. Kustov, **Russian Chemical Bulletin, International Edition 52**, 1928-1932 (2003).
22. M.N. Mikhailov and L.M. Kustov, **Russian Chemical Bulletin, International Edition 54**, 300-311 (2005).
23. İ. Önal and S. Şenkan, **Ind. Eng. Chem. Res. 36**, 4028-4032 (1997).
24. S. Özturk, İ. Önal and S. Şenkan, **Ind. Eng. Chem. Res. 39**, 250-258 (2000).
25. S.R. Blaszkowski, M.A.C. Nascimento and R.A. van Santen, **J. Phys. Chem. 100**, 3463-3472 (1996).
26. X. Zheng and P. Blowers, **Journal of Molecular Catalysis A: Chemical 229**, 77-85 (2005).
27. Y.V. Joshi and K.T. Thomson, **Catalysis Today 105**, 106-121 (2005).
28. M.S. Pereira and M.A.C. Nascimento, **Chemical Physics Letters 406**, 446-451 (2005).
29. S. Lillehaug, K.J. Børve, M. Sierka and J. Sauer, **J. Phys. Org. Chem. 17**, 990-1006 (2004).
30. W. Kohn and L.J. Sham, **Phys. Rev. 140**, A1133 (1965).
31. M.J. Frisch, G.W. Trucks, H.B. Schlegel, G.E. Scuseria, M.A. Robb, J.R. Cheeseman, J.A. Montgomery, Jr., T. Vreven, K.N. Kudin, J.C. Burant, J.M. Millam, S.S. Iyengar, J. Tomasi, V. Barone, B. Mennucci, M. Cossi, G. Scalmani, N. Rega, G. A. Petersson, H. Nakatsuji, M. Hada, M. Ehara, K. Toyota, R. Fukuda, J. Hasegawa, M. Ishida, T. Nakajima, Y. Honda, O. Kitao, H. Nakai, M. Klene, X. Li, J.E. Knox, H.P. Hratchian, J.B. Cross, C. Adamo, J. Jaramillo, R. Gomperts, R.E. Stratmann, O. Yazyev, A.J. Austin, R. Cammi, C. Pomelli, J.W. Ochterski, P.Y. Ayala, K. Morokuma, G.A. Voth, P. Salvador, J.J. Dannenberg, V.G. Zakrzewski, S. Dapprich, A.D. Daniels, M.C. Strain, O. Farkas, D.K. Malick, A.D. Rabuck, K. Raghavachari, J.B. Foresman, J.V. Ortiz, Q. Cui, A.G. Baboul, S. Clifford, J. Cioslowski, B.B. Stefanov, G. Liu, A. Liashenko, P. Piskorz, I. Komaromi, R.L. Martin, D.J. Fox, T. Keith, M.A. Al-Laham, C.Y. Peng, A. Nanayakkara, M. Challacombe, P.M.W. Gill, B. Johnson, W. Chen, M.W. Wong, C. Gonzalez and J.A. Pople, Gaussian 03, Gaussian, Inc., Pittsburgh PA, 2003.
32. A.D. Becke, **Phys. Rev. B 38**, 3098 (1988).
33. A.D. Becke and M.R. Roussel, **Phys. Rev. A 39**, 3761 (1989).
34. C. Lee, W. Yang and R.G. Parr, **Phys. Rev. B 37**, 785 (1988).
35. R.A. Van Santen and M. Neurock, "**Molecular Heterogeneous Catalysis**", Wiley, 2006.
36. J.J.P. Stewart, **J. Computer-Aided Molec. Design. 4**, 1 (1990).
37. R.A. Young, P.E. Mackie and R.B. von Dreele, **Journal of Applied Crystallography 10**, 262-269 (1977).
38. S.R. Blaszkowski and R.A. van Santen, **Topics in Catalysis 4**, 145-156 (1997).